The Journal of Immunology

RESEARCH ARTICLE | JUNE 01 2005

Respiratory Syncytial Virus Infection of Human Lung Endothelial Cells Enhances Selectively Intercellular Adhesion Molecule-1 Expression FREE

Ralf Arnold; ... et. al

J Immunol (2005) 174 (11): 7359–7367.
https://doi.org/10.4049/jimmunol.174.11.7359

Respiratory Syncytial Virus Infection of Human Lung Endothelial Cells Enhances Selectively Intercellular Adhesion Molecule-1 Expression

Ralf Arnold[1] and Wolfgang König

Respiratory syncytial virus (RSV) is worldwide the most frequent cause of bronchiolitis and pneumonia in infants requiring hospitalization. In the present study, we supply evidence that human lung microvascular endothelial cells, human pulmonary lung aorta endothelial cells, and HUVEC are target cells for productive RSV infection. All three RSV-infected endothelial cell types showed an enhanced cell surface expression of ICAM-1 (CD54), which increased in a time- and RSV-dose-dependent manner. By using noninfectious RSV particles we verified that replication of RSV is a prerequisite for the increase of ICAM-1 cell surface expression. The up-regulated ICAM-1 expression pattern correlated with an increased cellular ICAM-1 mRNA amount. In contrast to ICAM-1, a de novo expression of VCAM-1 (CD106) was only observed on RSV-infected HUVEC. Neither P-selectin (CD62P) nor E-selectin (CD62E) was up-regulated by RSV on human endothelial cells. Additional experiments performed with neutralizing Abs specific for IL-1α, IL-1β, IL-6, and TNF-α, respectively, excluded an autocrine mechanism responsible for the observed ICAM-1 up-regulation. The virus-induced ICAM-1 up-regulation was dependent on protein kinase C and A, PI3K, and p38 MAPK activity. Adhesion experiments using polymorphonuclear neutrophil granulocytes (PMN) verified an increased ICAM-1-dependent adhesion rate of PMN cocultured with RSV-infected endothelial cells. Furthermore, the increased adhesiveness resulted in an enhanced transmigration rate of PMN. Our in vitro data suggest that human lung endothelial cells are target cells for RSV infection and that ICAM-1 up-regulated on RSV-infected endothelial cells might contribute to the enhanced accumulation of PMN into the bronchoalveolar space. ***The Journal of Immunology,*** **2005, 174: 7359–7367.**

Respiratory syncytial virus (RSV)[2] is the major cause of serious lower respiratory disease in infancy and early childhood (1). By the age of 2 years >90% of children have been infected with RSV, and due to incomplete immunity, adults get reinfected throughout their life (2, 3). The epithelial cells of the respiratory mucosa are the primary target cells for RSV and evidence accumulated that they play an active role in the course of an ongoing RSV infection (4). Especially by the release of chemokines (5–7) and the expression of adhesion molecules, i.e., ICAM-1 (8–10), the lung epithelial cells contribute to the early acute inflammatory response evolving immediately postinfection. Obviously, the result of inflammation is dependent on viral and host cell factors. In this regard, we demonstrated the prominent role of the viral soluble G protein in modulating inflammatory responses of the host cell (11). Along the established chemotaxin gradient inflammatory effector cells are then chemotactically recruited from the local blood vessels via the mucosal tissue into the lumen of the alveolar space. Autopsy studies of infants who died following bronchiolitis revealed an intense peribronchial infiltration of mononuclear cells and cell debris in the airway lumen (12). Furthermore, a neutrophil-rich exudate detected by bronchoalveolar lavage has been described (13). These polymorphonuclear neutrophil granulocytes (PMN) adhere to the RSV-infected epithelial cells and become activated thereby (14, 15). As a consequence, they release reactive oxygen radicals and hydrolytic enzymes and, therefore, are responsible primarily for the subsequent intense inflammation of the lung (16, 17). The smaller airways then become plugged with cell debris and mucin.

Despite these basic insights into the mechanisms of an ongoing RSV infection, many aspects remain poorly understood. It is actually unknown whether human lung endothelial cells, which are intimately connected with the lung epithelium within the bronchoalveolar lumen, are also targets for RSV infection. It was reported by Haeberle et al. (18) that lung endothelial cells from RSV-infected mice expressed MIP-1α. However, whether this chemokine expression was directly induced by RSV infection or by means of a paracrine mechanism is still not known. The infection of HUVEC is still contradictorily discussed. Friedmann et al. (19) reported that RSV was not able to infect HUVEC or bovine thoracic aorta endothelium. In contrast, Visseren et al. (20) observed that RSV infection of HUVEC can occur and that infection increases their procoagulant activity. Because the activation of endothelial cells is one key process promoting the initiation of inflammatory reactions, which involve rolling, adhesion, and transmigration of leukocytes to the sites of inflammatory challenge, we asked whether human lung endothelial cells become infected with RSV and whether expression of adhesion molecules (CD62P, CD62E, CD54, CD106) might be directly modulated by RSV. Because evidence emerged that different endothelial cell types might show functional differences (21, 22), we analyzed HUVEC as a useful model because of their availability and reproduction, as well as human pulmonary lung aorta endothelial cells (HPAEC) and

Institute of Medical Microbiology, Otto-von-Guericke-University, Magdeburg, Germany

Received for publication November 4, 2004. Accepted for publication March 7, 2005.

The costs of publication of this article were defrayed in part by the payment of page charges. This article must therefore be hereby marked *advertisement* in accordance with 18 U.S.C. Section 1734 solely to indicate this fact.

[1] Address correspondence and reprint requests to Dr. Ralf Arnold, Institute of Medical Microbiology, Otto-von-Guericke-University, Leipzigerstrasse 44, 39120 Magdeburg, Germany. E-mail address: ralf.arnold@medizin.uni-magdeburg.de

[2] Abbreviations used in this paper: RSV, respiratory syncytial virus; F protein, fusion protein; HMVEC-L, human lung microvascular endothelial cell; HPAEC, human pulmonary lung aorta endothelial cell; m.o.i., multiplicity of infection; PKA, protein kinase A; PKC, protein kinase C; EGF-R, epidermal growth-factor receptor; EGM-2, endothelial growth medium-2; PMN, polymorphonuclear neutrophil granulocyte; MFI, mean fluorescence intensity.

0022-1767/05/$02.00

human lung microvascular endothelial cells (HMVEC-L) in our study. Our data demonstrate that all three endothelial cell types (HUVEC, HPAEC, and HMVEC-L) are permissive for a productive RSV infection and that they respond with an increased ICAM-1 cell surface expression subsequent to RSV infection. Consequently, cocultured PMN showed an increased adhesion as well as transmigration rate. These in vitro data suggest that human lung endothelial cells are productive target cells for RSV infection and that the prominent accumulation of inflammatory effector cells into the bronchioli of the RSV-infected lung is not only due to the chemotaxins released by the infected epithelial cells but also due to the direct up-regulation of ICAM-1 on RSV-infected lung endothelial cells. Thus, infection of lung endothelial cells by RSV may result in the activation of lung endothelia and in the augmentation of inflammatory processes.

Materials and Methods

Reagents, Abs, and cytokines

The following reagents were purchased: fibronectin, Hoechst stain 33258, human AB serum, and FITC-labeled albumin (Sigma-Aldrich); PI3K inhibitor L294002 (Biomol); MEK inhibitor PD98059, p38 MAPK inhibitor SB203580, protein kinase C (PKC) inhibitor (myristoylated epidermal growth-factor receptor (EGF-R) fragment (651–658)), protein kinase A (PKA) inhibitor KT5720, protein kinase G inhibitor sodium guanosine 3′,5′-cyclic monophosphorothioate, 8-bromo-, Rp-isomer (Rp-8-Br-cGMPs), and PMA (Calbiochem); JNK peptide inhibitor 1 (L-JNKI-1) (Alexis); PE-labeled mouse anti-human ICAM-1 mAb (clone: HA58), PE-labeled mouse anti-human VCAM-1 mAb (clone: 51-10C9), PE-labeled mouse anti-human CD62P mAb (P-selectin, clone: 9E1), PE-labeled mouse anti-human CD31 mAb (PECAM-1, clone: VP025), and all used FITC- and PE-labeled isotype control Abs (BD Biosciences); FITC-labeled mouse anti-human CD62E mAb (E-selectin, clone: 1.2B6) (Serotec); goat anti-human von Willebrand factor protein polyclonal Ab (Santa Cruz Biotechnology); anti-fusion protein (F protein) mAb (clone: 9C5) (Hytest); Cy3-labeled AffiniPure goat anti-mouse IgG (H + L) and FITC-labeled AffiniPure rabbit anti-goat IgG (H + L) (Dianova); HRP-conjugated rabbit anti-mouse IgG (DakoCytomation); blocking mAbs: a-IL-1β (clone: 8516.311), a-IL-1α (clone: 4414.141), a-IL-6 (clone: 6708.111), a-TNF-α (clone: 1825.12), a-ICAM-1 (clone: BBIG-I1 (11C81)), a-VCAM-1 (clone: BBIG-VI (4B2)), unspecific IgG1-isotype control and human rTNF-α (R&D Systems); PBS, HBSS, endothelial growth medium-2 (EGM-2)-and EGM-2-MV-Bulletkit-medium (Cambrex/Clonetics); FCS (Biochrom AG Seromed); tetrazolium salt 4-[3-(4-iodophenyl)-2-(4-nitrophenyl)-2H-5-tetrazolio]-1,3-benzene disulfonate assay (Roche). If not stated otherwise, all other media and supplements were obtained from Invitrogen Life Technologies. Cell culture plastic material was obtained from Greiner Labortechnik and all fine chemicals were supplied by Sigma-Aldrich.

Cells

Endothelial cell culture. HUVEC were harvested from umbilical cords by collagenase perfusion (0.1% in PBS) (23). HUVEC were used for the experiments at passage levels three to five. The cultures stained uniformly positive for EC markers (CD31 and von Willebrand factor). HMVEC-L and HPAEC cryopreserved as secondary cultures were purchased from Cambrex/Clonetics. HUVEC and HPAEC were cultured in complete endothelial cell growth medium (EGM-2 BulletKit (2% FCS)), and HMVEC-L was cultured in complete EGM-2-MV (EGM-2-MV-BulletKit (5% FCS)) medium. To support cell attachment and growth, tissue culture flasks and plastic plates were precoated with fibronectin (10 μg/ml) for 30 min at 37°C. HMVEC-L and HPAEC were used from three different donors at passages three through seven. The endothelial cells were passaged by short trypsinization (0.05% trypsin/5 mM EDTA).

PMN isolation. Immediately before each experiment peripheral blood was obtained from healthy volunteers. Blood was collected in sodium-heparin tubes, and PMN were isolated using a single-step gradient (Polymorphprep; Nycomed). Contaminating erythrocytes were lysed by hypotonic shock (155 mM NH_4Cl, 10 mM $KHCO_3$, and 0.1 mM EDTA). The final PMN suspension (>95% neutrophils) were washed two times and resuspended in HBSS.

Virus growth and preparation

The Long strain of RSV (American Type Culture Collection (ATCC)) was propagated and titrated in HEp-2 cells (ATCC). HEp-2 cells were cultured in DMEM (5% FCS, 2 mM glutamine, 4500 mg/L D-glucose, streptomycin (100 μg/ml), penicillin (100 U/ml)). Cell cultures and prepared virus stocks were free of mycoplasmic contamination routinely verified by a DNA staining method using Hoechst 33258 stain solution (24). Confluent monolayers of HEp-2 cells were infected with RSV for 3 h (multiplicity of infection (m.o.i.) = 0.1) in DMEM. The monolayers were washed, overlaid with DMEM (0.5% FCS) and incubated at 37°C in 5% CO_2 atmosphere until the cytopathic effect reached ~80%. Thereafter, the supernatants were harvested and cellular debris was removed by centrifugation (5000 × g, 10 min). RSV was concentrated by polyethylene glycol precipitation (10%) and purified by means of discontinuous sucrose gradient centrifugation (25). To stabilize the purified virus particles they were resolved in 20% sucrose/NT-buffer (150 mM NaCl, 50 mM Tris-HCl, pH 7.5) and stored at −80°C. Stock titer of the used virus pool was adjusted to 10^8 PFU/ml.

RSV titration

For virus titration, cell supernatants and prepared RSV stock solutions were diluted serially 10-fold onto confluent HEp-2 monolayers cultured in 96-well flat-bottom plates. The virus titer was quantified using the microplaque immunoperoxidase method (26).

Cell infection and stimulation

Endothelial cells were grown in monolayers in 12-well plates. The virus stock was diluted with culture medium and endothelial cells were infected at a m.o.i. of 0.5–5. For control experiments RSV was inactivated by UV light irradiation on ice for 20 min. The complete inactivation was determined by the absence of plaque formation of UV-treated RSV. Confluent monolayers of endothelial cells were washed with medium without additives (basal medium), exposed to RSV for 2 h in a volume of 400 μl of basal medium, washed, and incubated with fresh complete medium for the desired incubation times at 37°C at 5% CO_2 atmosphere. Cells were harvested at various times after RSV infection and analyzed for adhesion molecule expression by FACS analysis. In the course of blocking experiments, the inhibitors (LY294002, RP-8-Br-cGMP, PKC inhibitor myristoylated EGF-R fragment, KT5720, SB203580, PD98059, L-JNKI-1) were added 30 min before RSV infection in basal medium. Compounds were stored in DMSO at −80°C. At the day of the experiment, they were freshly diluted in basal EGM-2 medium and added to the cells with a final DMSO concentration <0.1%. RSV was then added and infection was performed for 2 h. Thereafter, monolayers were aspirated and 3 ml of fresh complete endothelial cell medium supplemented with the indicated inhibitors was added. Cell viability was measured by a microplate reader (Tecan) using a modified MTT assay (tetrazolium salt 4-[3-(4-iodophenyl)-2-(4-nitrophenyl)-2H-5-tetrazolio]-1,3-benzene disulfonate assay according to the instructions of the manufacturer). At the concentrations used, the added pharmacological inhibitors induced no cytotoxicity. Harvested cells were immediately stained for FACS analysis. To analyze autocrine mechanisms cytokine blocking Abs (10 μg/ml) were directly added to the cells following RSV infection.

FACS staining

The cells were prepared for FACS analysis essentially as described earlier (27). Endothelial cells were harvested by short incubation with trypsin/EDTA on ice. The trypsinization was stopped by addition of the same volume of PBS (10% FCS, 0.1% NaN_3). Cells were washed two times in PBS, and cells (5×10^5) were stained for 1 h at 4°C either with the mAbs specific for ICAM-1, VCAM-1, CD62E, CD62P (10 μg/ml), or with isotype matched control IgG Abs. All Abs were primary labeled. To determine productive RSV infection of endothelial cells, the cells were analyzed for cell surface expression of viral F protein. Binding of anti-F protein Ab was visualized with a second staining using Cy3-labeled goat anti-mouse IgG. After cell washing, the cell bound fluorescence signal was determined by FACSCalibur (BD Biosciences). The data are presented as mean fluorescence intensity (MFI) of 10,000 cells after subtraction of background staining (IgG isotype control) or as percent of adhesion molecule expressing cells, reflecting percents of cells with fluorescence above control (1%). Data were analyzed by means of CellQuest software (BD Biosciences).

RT-PCR analysis of ICAM-1

The total cellular RNA from uninfected, and RSV-infected endothelial cells (5×10^5) was extracted using Trifast reagent (PeqLab) according to the manufacturer's instructions. For the synthesis of cDNA, prepared total RNA (2 μg) was mixed with Moloney murine leukemia virus reverse transcriptase buffer (3 mM $MgCl_2$, 75 mM KCl, 50 mM Tris-HCl; Life Technologies), 0.5 mM deoxyribonucleoside triphosphates (dNTP-Set; Life

Technologies), 1 U/μl RNase inhibitor (Amersham), 4 U/μl Moloney murine leukemia virus reverse transcriptase (Life Technologies), and 2.0 ng of oligo(dT)$_{12-18}$ in a volume of 50 μl. The synthesis of cDNA was done by heating at 37°C for 60 min. The cDNA was stored at −20°C. Aliquots of 2.5 μl of the synthesized cDNA (100 ng of RNA) were mixed with a 22.5 μl of PCR mixture containing 2.5 μl of 10× PCR buffer (15 mM $MgCl_2$; Life Technologies), 2 μl of deoxynucleotides (400 nM each), 1 μl of 3′- and 5′-specific primers (200 nM each) and 0.25 μl of TaqDNA polymerase (5 U/μl; Qiagen). The expression of the housekeeping gene GAPDH served as an internal standard, the GAPDH primers (sense 5′-ACCA CAAGTCCAATGCCATCAC-3′, antisense 5′-TCCACCACCCTGTTGC TGTA-3′) were synthesized by Metabion. Amplification was initiated with denaturation for 4 min at 94°C. Cycling conditions were as follows: 33 cycles at 94°C for 45 s, 55°C for 45 s, and 72°C for 45 s with a final amplification at 72°C for 10 min using a DNA thermal cycler (Primus 95plus; MWG Biotec). The primers specific for ICAM-1 plus ICAM-1-positive control were supplied by R&D, and PCR was performed according to the manufacturer's instruction. The yielded PCR products with expected sizes of 420 bp (GAPDH), 750 bp (ICAM-1), and 320 bp (positive control) were run on 1.2% agarose gel with DNA m.w. marker XIV (100-bp ladder; Roche). Thereafter, adequacy of RNA loading was determined by ethidium bromide staining and UV illumination. Densitometry was performed using a Lumi-Imager F1 Workstation equipped with LumiAnalyst version 3.1 (Roche).

Adhesion assay

The adhesion of PMN and PMA-activated U937 cells (ATCC) to confluent monolayers was determined by measuring the fluorescence signal of adherent cells fluorescently labeled with the acetyloxymethylester of calcein, calcein-AM (Calbiochem) (28). Before adhesion, U937 cells were differentiated with PMA (50 ng/ml) overnight. Confluent endothelial monolayers grown in a 96-well flat-bottom plate were overlaid with 4×10^5 cells in 50 μl of medium. In case of blocking experiments, monolayers were preincubated with a-ICAM, a-VCAM-1, or unspecific IgG1 (20 μg/ml) for 30 min and FcγR on PMN were additionally blocked by prior incubation with 50% human AB serum (Sigma-Aldrich) for 15 min. Monolayers and PMN were washed two times. The cells were allowed to attach for 30 min at 37°C. Then, unbound cells were removed by flicking and washing the plates three times. Residual fluorescence was measured using a SpectraFluorPlus Reader (Tecan). To determine the linearity between cell number and fluorescence signal, standard curves were pipetted in 96-well plates on the day of the experiment. Linearity was given up to 8×10^5 cells. Adhesion was calculated as the ratio of cells adherent to RSV-infected endothelial cells compared with cells adherent to sham-infected cells.

Transendothelial migration of PMN

Endothelial cells (HUVEC, HMVEC-L, HPAEC; 3×10^5 cells/ml) were cultured on fibronectin-coated Transwell inserts (10 mm diameter polycarbonate membrane with 8 μm pores; Nunc). Medium was only added into the upper compartment to inhibit the formation of bilayers. Monolayers formed within 2–3 days. Their confluence was determined by measuring the permeability for FITC-labeled albumin. The monolayers were expected to be confluent and used when diffusion of albumin was <5% of equilibrium. The monolayers were infected with RSV (m.o.i. = 5) and incubated for 48 h. Thereafter, inserts were washed with PBS, transferred into fresh 24-well plates (Greiner), and checked again for their confluence. PMN (2×10^5/200 μl) were added to the upper compartment and medium containing IL-8 (10 ng/ml) was added to the lower compartment. The plates were incubated for 3 h at 37°C and 5% CO_2. Thereafter, the plates were centrifuged to dislodge migrated cells still adherent to the bottom of the filters. An investigator blinded to the protocol assessed the number of migrated cells in quadruplicate by hemocytometer, and percent migration was determined. The transmigration rate of PMN via noninfected cells was assigned 100%. Calculating the percentage of transmigration allowed a comparison of replicate experiments.

Statistics

If not stated otherwise, the results obtained by flow cytometry studies are presented as means and SEM (MFI ± SEM) or percentage of cells ± SEM. The significance was evaluated by two-sided Student's *t* test.

Results

RSV infection of human endothelial cells

To analyze whether human endothelial cells are targets for RSV infection, we infected HUVEC, HMVEC-L, and HPAEC with RSV. The replication of RSV was determined by analyzing the expression of the virus F protein on the cell surface of infected endothelial cells by FACS analysis. As shown in Fig. 1*A1*, HUVEC expressed the viral F protein after 24 h postinfection on their cell surfaces. Only the addition of infectious virus particles led to the expression of cell surface F protein. In contrast, virus particles inactivated by UV irradiation were not able to induce any F protein expression (Fig. 1, *A1* and *B*). Therefore, virus replication was a prerequisite for the expression of F protein on HUVEC cells. Similar results were obtained with an Ab specific for the G protein (data not shown). When an isotype-matched control Ab was used in place of the mAb specific for the F protein, cells that had been infected with RSV did not stain positive. Similar fluorescence histograms were obtained with noninfected cells stained with anti-F protein mAb (Fig. 1*A1*, dashed line). The maximal expression of F protein was determined on HUVEC 24 h subsequent to infection. Additional infection studies performed with HUVEC verified that the expression of F protein increased in a time- and RSV-dose-dependent manner during the first 24 h postinfection (Fig. 1*B*). When we analyzed the F-protein expression on RSV-infected HPAEC, we observed a similar expression pattern (data not shown). In contrast, HMVEC-L infected with RSV did not stain positive for F protein during the first 24 h following infection. However, thereafter, the expression of F protein increased steadily and reached its maximum after 72 h postinfection (Fig. 1*A2*). Beyond an incubation time of 72 h, all infected endothelial cell cultures showed increasing cytopathic effects and cell death occurred. During our performed experiments we observed no apoptotic cell processes determined by microscopic analysis instead of necrotic cell death in RSV-infected endothelial cell cultures. To determine whether the infection of endothelial cells resulted in the release of new infectious progeny virus, the cell supernatants were titrated. As depicted in Fig. 1*C*, all three endothelial cell types produced new progeny virus. Especially the infection of HMVEC-L led to a prominent release of new infectious RSV particles. For control, when supernatants were titrated as early as 12 h postinfection, no infectious particles were found. Therefore, the primary addition of RSV does not account for the progeny virus determined after 48 h.

Enhanced ICAM-1 expression on HUVEC, HPAEC, and HMVEC-L infected with RSV

We and others observed enhanced ICAM-1 cell surface expression on lung epithelial cells infected with RSV (4, 8–10). Thus, we thought to determine whether infection of endothelial cells resulted in an increased expression of adhesion molecules. As can be seen from Fig. 2, all three endothelial cell types expressed ICAM-1 constitutively at levels well above background. Compared with HUVEC and HMVEC-L, the HPAEC showed the highest constitutive ICAM-1 cell surface expression (Fig. 2*B*). When cells were infected with RSV, the ICAM-1 cell surface expression increased significantly on all three endothelial cell types in a time-dependent manner.

As early as 24 h postinfection, an increased ICAM-1 expression was observed on HUVEC and HPAEC. This expression of ICAM-1 increased steadily with prolonged incubation time up to 72 h (Fig. 2, *A* and *B*). Thereafter, expression declined due to increasing cytotoxicity (data not shown). Similar to the delayed F protein expression observed on RSV-infected HMVEC-L, we obtained no significant up-regulation of ICAM-1 on these cells during the first 24 h postinfection (Fig. 2*C*). Thereafter, the increasing F protein expression paralleled the RSV-induced up-regulation of ICAM-1 on HMVEC-L up to 96 h postinfection. Subsequently, cell cytotoxicity increased and ICAM-1 expression declined (data

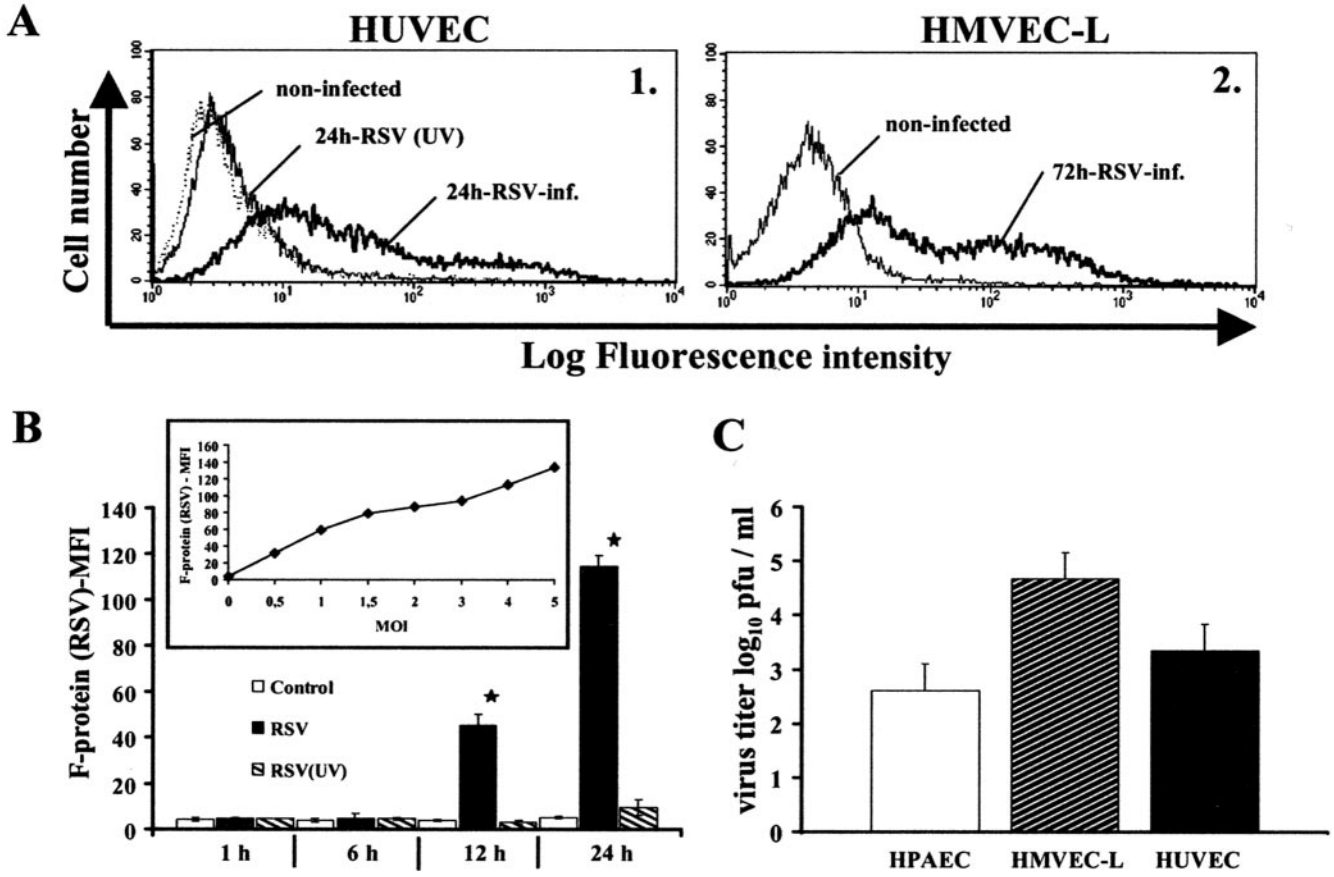

FIGURE 1. Productive infection of human endothelial cells with RSV. The cell surface expression of virus F protein was determined by FACS analysis. *A*, Data are represented as overlaid distribution histograms of surface fluorescence intensity from stained virus F protein on HUVEC (1) and HMVEC-L (2) infected with RSV (m.o.i. = 5). *1,* F protein expression on noninfected HUVEC (dashed line); on cells exposed to UV-irradiated noninfectious RSV (RSV-UV) (thin line), and on RSV-infected cells 24 h postinfection (thick line). *2,* F protein expression on noninfected HMVEC-L (thin line) and on RSV-infected HMVEC-L 72 h postinfection (m.o.i. = 5) (thick line). Histograms are representative of multiple experiments. *B*, Time course of F protein expression on HUVEC infected with RSV (m.o.i. = 5) and UV-inactivated RSV, respectively. Results are means ± SEM from four independent experiments. Significant differences from noninfected cells (□) are indicated by ∗, $p < 0.01$. *Inset,* Intensity of F-protein expression on HUVEC infected with RSV at different m.o.i. for 24 h. *C*, Release of infectious RSV particles into the cell supernatants of HPAEC, HMVEC-L, and HUVEC 48 h postinfection with RSV (m.o.i. = 3). Supernatants were harvested and RSV titers were determined by immunoplaque assay in HEp-2 cells. Results ± SEM ($n = 3$) are presented as mean titers ($\log_{10}$ PFU per milliliter).

not shown). When RSV-induced ICAM-1 expression was directly compared between the different endothelial cell types, HUVEC expressed the most increased ICAM-1 cell surface expression (Fig. 2*A*).

The addition of nonreplicative UV-inactivated RSV did not induce ICAM-1 expression beyond the constitutive expression level (data not shown) suggesting that productive infection of all three endothelial cell types under investigation was a prerequisite for the observed RSV-dependent ICAM-1 up-regulation.

In contrast to ICAM-1, we observed that the expression of selectins (CD62P, CD62E) was not inducible by RSV neither on HUVEC nor on HMVEC-L and HPAEC, respectively (data not shown).

Enhanced VCAM-1 expression only on RSV-infected HUVEC

Recently, the enhanced expression of VCAM-1 on RSV-infected A549 cells was reported (29). When we analyzed endothelial cells for VCAM-1 expression they did not stain constitutively positive for VCAM-1. Subsequent to RSV infection, only HUVEC up-regulated VCAM-1 on their cell surface 24 h after their infection. This expression increased with prolonged incubation time up to 72 h (Fig. 3*A*). The maximal percentage of VCAM-1-positive cells was observed after 72 h postinfection (Fig. 3, *A* and *B*). Although a m.o.i. of 5 was used throughout these infection studies, HUVEC stained only positive for VCAM-1 in the range of 30%. Similar to ICAM-1 expression, the addition of noninfectious virus (m.o.i. = 5, inactivated by UV-irradiation) did not induce VCAM-1 expression on HUVEC (data not shown). To verify that the HUVEC under study were still able to up-regulate VCAM-1 in a TNF-α-dependent manner, peaking at 4–6 h, we determined VCAM-1 in our in vitro cell culture system on HUVEC activated with TNF-α. As shown in Fig. 3*C*, HUVEC showed a significant VCAM-1 expression after 6 h following TNF-α stimulation.

Cellular ICAM-1 mRNA amount is increased in RSV-infected endothelial cells

To study the RSV-induced ICAM-1 expression in more detail, we performed RT-PCR experiments. In HPAEC, transcripts for ICAM-1 were detectable only at low levels in noninfected cells (Fig. 4, *lane 1*) but RSV infection induced enhanced message levels in a dose-dependent manner (compare *lane 1* with *lanes 2–6*). When compared with noninfected cells (*lane 1*), the amount of cellular ICAM-1 mRNA was most prominent in cells infected with

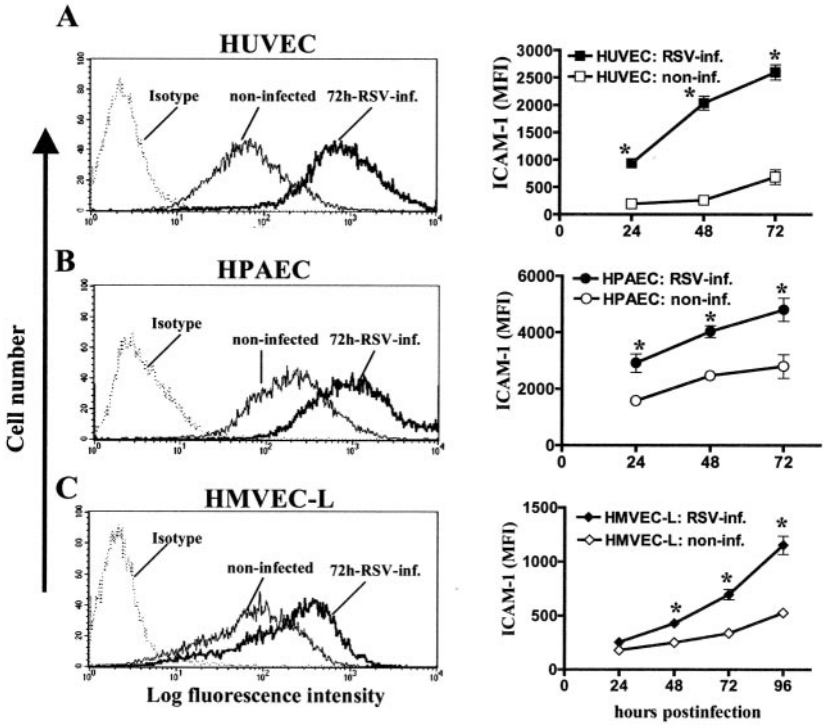

FIGURE 2. Enhancement of ICAM-1 cell surface expression on RSV-infected human endothelial cells. ICAM-1 expression on HUVEC (*A*), HPAEC (*B*), and HMVEC-L (*C*) was determined by FACS analysis 24–72 h/96h postinfection (m.o.i. = 5). *Left,* Representative FACS histogram overlays of log mean fluorescence frequency distribution of 10,000 cells are depicted; dashed line: IgG1 isotype control; thin line: constitutive ICAM-1 expression on noninfected cells cultured for 72 h; thick line: ICAM-1 expression on RSV-infected cells 72 h postinfection. *Right,* Comparison of kinetics of ICAM-1 expression on endothelial cells infected with RSV (m.o.i. = 5) (closed symbols) or noninfected (open symbols). Results are means ± SEM ($n = 4$). Significant differences from noninfected cells (open symbols) are indicated by ∗, $p < 0.01$.

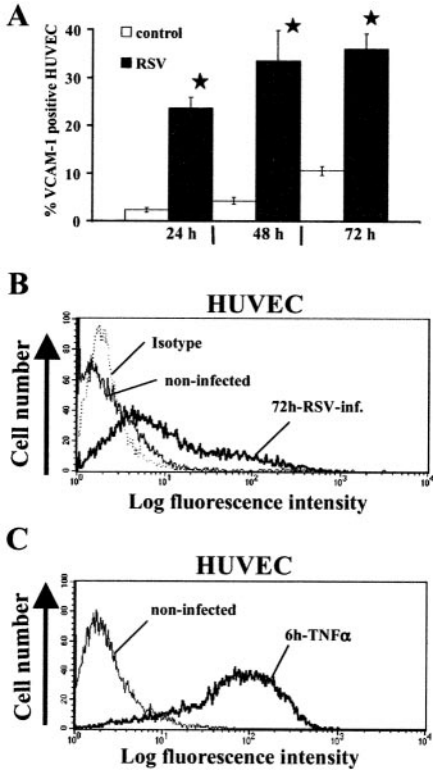

FIGURE 3. VCAM-1 cell surface expression on RSV-infected HUVEC. *A*, Percentage of VCAM-1-positive HUVEC subsequent to RSV infection (m.o.i. = 5) determined by FACS analysis. Results are means ± SEM ($n = 4$). Significant differences from sham-infected cells (□) are indicated by ∗, $p < 0.01$. *B*, Representative fluorescence overlay histogram showing de novo VCAM-1 expression on HUVEC 72 h subsequent to RSV infection (m.o.i. = 5); IgG1 isotype control (dashed line), constitutive expression of VCAM-1 on cells cultured for 72 h (thin line), RSV-induced VCAM-1 expression (thick line). *C*, Representative overlay histogram showing de novo VCAM-1 expression on HUVEC stimulated with TNF-α (10 ng/ml); constitutive expression of VCAM-1 after 6 h incubation time (thin line), VCAM-1 expression on HUVEC activated with TNF-α for 6 h (thick line).

RSV at a m.o.i. of 5 (*lane 6*). Exposure of HPAEC to nonreplicative virus (RSV-UV) did not increase the amount of ICAM-1 mRNA when compared with noninfected cells (*lane 1* and *7*). To verify inherent PCR specificity, a positive control, supplied by the manufacturer, was amplified in parallel and resulted in a visible band of 320 bp in size (*lane 8*). Similar results showing an enhanced amount of cellular ICAM-1 mRNA were obtained when HUVEC and HMVEC-L were infected with RSV (data not shown).

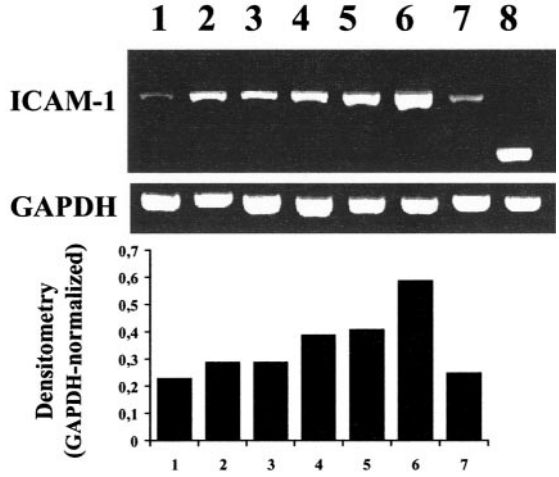

FIGURE 4. RSV infection of HPAEC induced an increased cellular amount of ICAM-1 mRNA. Cellular amount of mRNA for ICAM-1 and GAPDH determined by RT-PCR. Cells were infected with different m.o.i. and cultured for 12 h. The *top panel* shows the cellular amount of mRNA expression of ICAM-1 (750 bp) and GAPDH (420 bp) determined by RT-PCR. *Lane 1,* Control; *lane 2,* RSV (m.o.i. = 0.5); *lane 3,* RSV (m.o.i. = 1); *lane 4,* RSV (m.o.i. = 2); *lane 5,* RSV (m.o.i. = 3); *lane 6,* RSV (m.o.i. = 5); *lane 7,* RSV-UV (m.o.i. = 5); *lane 8,* positive PCR-control (320 bp in size). The *bottom panel* shows laser densitometry analysis of ICAM-1 bands that were normalized to GAPDH bands. The results are representative of multiple experiments.

RSV-induced expression of ICAM-1 and VCAM-1 is not mediated by an autocrine mechanism

It is well known that ICAM-1 and VCAM-1 are markedly up-regulated on endothelial cells by the proinflammatory cytokines TNF-α and IL-1β, respectively (30, 31), and that HUVEC and microvascular endothelial cells are able to secrete a variety of cytokines (32). Therefore, we hypothesized that RSV-induced expression of ICAM-1 and VCAM-1 is partly mediated by an autocrine mechanism as it was reported for A549 epithelial cells (33). However, we observed no cytokine (IL-1α, IL-1β, IL-6, and TNF-α)-mediated up-regulation of ICAM-1 on HUVEC and HPAEC. In addition, VCAM-1 expression on HUVEC 24 h postinfection was also not mediated by an autocrine mechanism (data not shown).

RSV induces ICAM-1 expression in a PI3K-, PKA and PKC-, and p38 MAPK-dependent manner

We next used pharmacological inhibitors to investigate whether RSV-dependent ICAM-1 expression on HUVEC might be mediated through the activity of one or more intracellular signaling pathways. Recently, evidence accumulated that activation of the PI3K (34), the ERK1/ERK2 (35), and the PKC (36) occur in RSV-infected human epithelial cells. Therefore, we asked whether the activity of intermediate kinases might be a prerequisite for the RSV-induced expression of ICAM-1 on HUVEC. We analyzed HUVEC because ICAM-1 was most markedly up-regulated on these cells. Cell monolayers were pretreated with these inhibitors for 30 min, infected with RSV and then incubated in the presence of these pharmacological substances for further 48 h. As can be seen from Fig. 5, the exposure of HUVEC with the PI3K inhibitor Ly294002 inhibited nearly completely the RSV-induced ICAM-1 up-regulation. Furthermore, inhibition of the PKC by means of the myristoylated EGF-R inhibitor peptide as well as inhibition of PKA activity by KT5720, respectively, inhibited significantly the RSV-induced ICAM-1 up-regulation. In contrast, inhibition of the protein kinase G through the specific inhibitor RP-8-Br-cGMP did not modulate ICAM-1 expression. With regard to MAPK signaling pathways, we determined the effect of the MEK-1 inhibitor PD98059, the JNK peptide inhibitor 1 (L-JNKI-1), and the p38 MAPK inhibitor SB203580 on RSV-induced ICAM-1 expression. As shown, only the inhibition of the p38 MAPK cascade through SB203580 diminished the cell surface ICAM-1 expression on RSV-infected HUVEC in a significant manner. The involvement of p38 kinase activity was further substantiated by analyzing a second specific p38 kinase inhibitor, i.e., 2-(4-chlorophenyl)-4-(4-fluorophenyl)-5-pyridin-4-yl-1,2-dihydropyrazol-3-one used at a concentration of 1 μM. Similar data were obtained (data not shown).

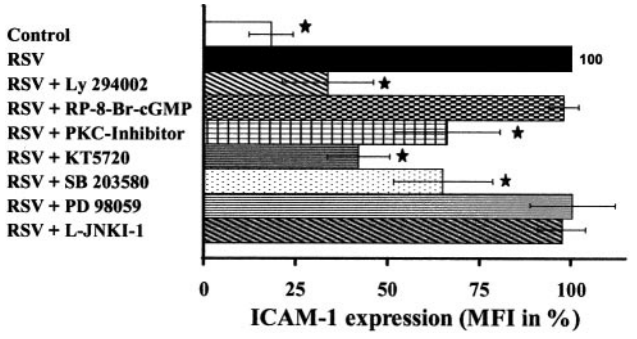

FIGURE 5. Signaling pathways involved in RSV-dependent ICAM-1 expression on HUVEC. Cells were pretreated with vehicle (control), Ly294002 (6.4 μM), RP-8-Br-cGMP (20 μM), PKC inhibitor (myristoylated EGF-R fragment; 20 μM), KT5720 (400 nM), SB203580 (1 μM), PD98059 (5 μM), or L-JNKI-1 (20 μM) for 30 min before the infection with RSV. After infection, cells were washed and incubated in the presence of the inhibitors for 36 h. The MFI of ICAM-1 expression on RSV-infected cells was designated as 100% and data are represented as a percentage of this value. Results are means ± SEM ($n = 5$); *, $p < 0.05$, significant vs RSV-infected cells.

RSV infection of endothelial cells induces adhesion of PMN and U937 cells

A leukocyte adhesion assay was performed to investigate whether the RSV-induced ICAM-1 expression on HUVEC, HMVEC-L and HPAEC might be responsible for an increased adhesion of immune effector cells. For this purpose, RSV-infected endothelial cell monolayers were cocultured with PMA-activated U937 cells, a promyelocytic cell line, and PMN, respectively. Infection of all three endothelial cell types with RSV induced at least a 2-fold increase in the adhesion of U937 cells and PMN (Fig. 6*A*). Furthermore, with regard to HMVEC-L the adhesion of U937 cells increased 3-fold compared with noninfected cells, and PMN were 5-fold more adherent to RSV-infected HUVEC when compared

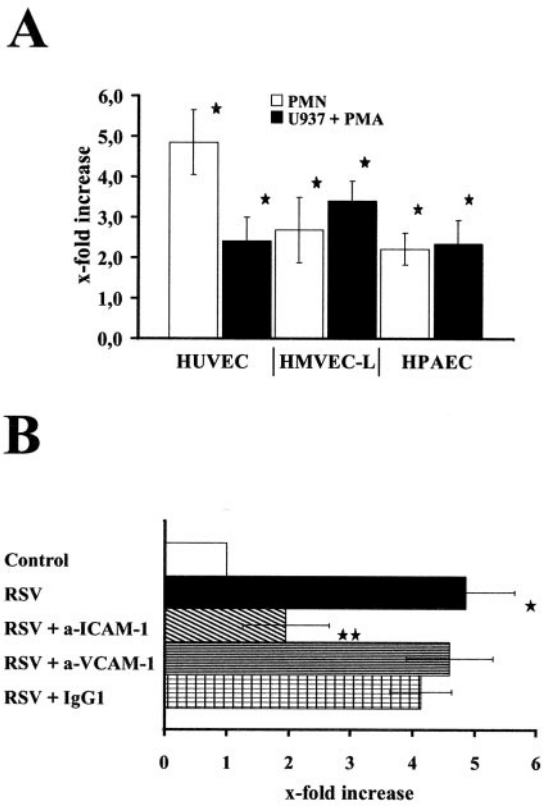

FIGURE 6. Adhesion of PMN and PMA-activated U937 cells to RSV-infected human endothelial cells. *A*, Monolayer of endothelial cells were cocultured with PMN (□) and U937 cells (■) 48 h postinfection, and adhesion of effector cells was determined after 30 min. Adhesion was calculated as the ratio of cells adherent to RSV-infected endothelial cells compared with cells adherent to sham-infected cells. Results are means ± SEM ($n = 3$); *, $p < 0.05$, significant increase with RSV infection. *B*, Role for ICAM-1 and VCAM-1 in adhesion of PMN to HUVEC. RSV-infected HUVEC were pretreated with blocking Abs specific for ICAM-1 (20 μg/ml), VCAM-1 (20 μg/ml), or IgG1 isotype control (20 μg/ml). Adhesion was calculated as the ratio of cells adherent to RSV-infected endothelial cells compared with cells adherent to sham-infected cells. Results are means ± SEM ($n = 6$); *, $p < 0.05$, significant increase with RSV vs sham-infected cells; **, $p < 0.05$ significant decrease compared with RSV-infected cells cultured without blocking Ab.

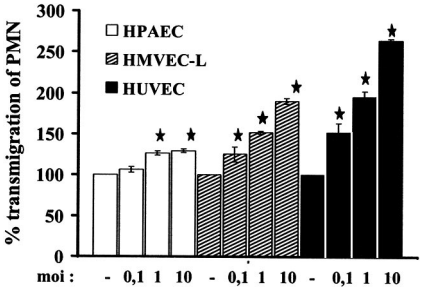

FIGURE 7. Effect of RSV infection on PMN transmigration. Confluent endothelial cell monolayers were infected with RSV (m.o.i. = 0.1, 1, 10) and incubated for 48 h. Purified PMN were plated onto these monolayers in the upper well of a Transwell. The IL-8 (10 ng/ml) was added to the lower well and the transmigration was measured after 3 h of culture time. Results are means ± SEM ($n = 3$) and are presented as percents of PMN migrated through sham-infected cells, which was assigned 100%; ∗, $p < 0.01$, significant vs sham-infected cells.

with noninfected cells. To analyze whether the observed increased ICAM-1 cell surface expression might be responsible for the increased adhesion rate of PMN to RSV-infected HUVEC, we cocultured PMN in the presence of blocking mAb specific for ICAM-1, VCAM-1, or isotype IgG1 Ab. As shown in Fig. 6*B*, preincubation of the monolayers with specific blocking ICAM-1 mAb diminished the adhesion rate of PMN from 5- to 2-fold compared with noninfected cells. In contrast, with regard to the adhesion of PMN blocking of VCAM-1 or addition of isotype control IgG1 Ab was without any influence. Therefore, ICAM-1 up-regulated on RSV-infected endothelial cells showed functional integrity.

RSV infection of endothelial cells results in higher transmigration rates of PMN

To determine whether the increased adhesion of PMN to RSV-infected endothelial cells might result in an increased transmigration rate, confluent endothelial cell monolayers, grown on polycarbonate filters, were cocultured with purified PMN. The PMN were allowed to settle and migrate for 3 h across noninfected and RSV-infected intact endothelial cell monolayers. To provide a chemotactic gradient for the cocultured PMN, the medium of the lower well compartment contained the chemotaxin IL-8 at a concentration of 10 ng/ml. This in vitro transmigration model should mimic the IL-8 chemotaxin gradient established by the RSV-infected lung epithelial cell in the course of an ongoing RSV infection. As depicted in Fig. 7, migration of PMN across RSV-infected monolayers, regardless of the endothelial type used, was significantly enhanced when compared with noninfected monolayers. The transmigration rate increased always in a RSV-dose-dependent manner. However, the RSV-induced transmigration rate differed with respect to the endothelial cell type used; the order of potency was: HUVEC > HMVEC-L > HPAEC.

Discussion

Following RSV infection, an increased number of immune effector cells accumulate in the lung tissue and airway lumen (12). Everard et al. (13) reported that PMN accounted for 93 and 76% of the cells recovered by BAL from central and peripheral airways of infants suffering from RSV bronchiolitis. However, detailed knowledge elucidating the RSV-induced recruitment of immune effector cells as well as development of the inflammatory response is failing.

In the case of RSV infection of the lower respiratory tract, the microvascular endothelial cells of the pulmonary capillaries are in intimate contact with the RSV-infected lung epithelial cells. Our data presented in this study report for the first time that primary lung endothelial cells (HMVEC-L, HPAEC) and HUVEC are target cells for RSV infection. The cells expressed viral F protein on their cell surface and shed infectious progeny virus into the cell supernatant. These results are in agreement with data recently published by Visseren at al. (20) showing that HUVEC are permissive for RSV infection and respond thereafter with an increased procoagulant activity.

Our data show that subsequent to RSV infection all three endothelial cell types up-regulated their ICAM-1 expression in a time- and virus-load-dependent manner. Similar to A549 cells replication of RSV was always a prerequisite for ICAM-1 up-regulation on all three endothelial cell types (data not shown for HMVEC-L and HPAEC).

It has been shown by Chini et al. (37) that the enhanced expression of ICAM-1 on RSV-infected lung epithelial cells was dependent on novel mRNA synthesis. They supplied evidence that the NF-κB and C/EBP binding sequences located in the ICAM-1 promoter are required for RSV-induced up-regulation of ICAM-1. Similar to RSV-infected lung epithelial cells we observed an increased amount of cellular ICAM-1 mRNA in endothelial cells infected with RSV suggesting that the enhanced cell surface expression of ICAM-1 is primarily mediated via an increased gene transcription activity and de novo protein synthesis. In this regard, when RSV-infected endothelial cells were cultured in the presence of actinomycin D (5 μg/ml), aspirin (1 mM), or cycloheximide (10 μg/ml) the RSV-induced ICAM-1 up-regulation was substantially inhibited (data not shown).

The release of IL-1α from RSV-infected A549 lung epithelial cells is well recognized for its pivotal role in mediating ICAM-1 expression in an autocrine manner (33) as well as for its paracrine ICAM-1 inducing effect on HUVEC (38). Our data presented in this study indicate that neither IL-1α, IL-1β, IL-6, nor TNF-α, possibly secreted from infected endothelial cells, are responsible for the up-regulation of ICAM-1 on RSV-infected HUVEC and HPAEC, respectively.

Beside the RSV-induced up-regulation of ICAM-1 we observed no up-regulation of selectins and VCAM-1 on RSV-infected human HMVEC-L and HPAEC up to 24 h postinfection. Only, RSV-infected HUVEC expressed VCAM-1 on their cell surface 24 h postinfection, but similar to primary lung endothelial cells no up-regulation of selectins was observed. In contrast to the postcapillary venules of the systemic circulation, where PMN emigration normally occurs, the pulmonary capillaries are the primary site of emigration in the pulmonary circulation and rolling does not occur (39). Due to the size of the vascular diameter, the PMN are trapped within the capillaries. Therefore, an increased expression of selectins seems not to be a prerequisite for the extravasation of PMN out of the pulmonary capillaries. Trapped PMN, additionally activated via soluble proinflammatory mediators, i.e., chemotaxins, as well as cell-cell interactions, become enlarged and more rigid, thereby increasing their retention in the lung capillaries.

All leukocytes use the β_2-integrin/ICAM-1 interaction for adhesion and transmigration. In this study we observed an increased adhesion of PMN and monocytic cells (PMA-activated U937 cells) to RSV-infected endothelial cells. For PMN, we verified that this increased adhesion was dependent on the increased cell surface amount of ICAM-1. We hypothesize that leukocytes migrating out of the bloodstream into the pulmonary circulation of the RSV-infected lung become additionally activated by soluble inflammatory mediators in a paracrine fashion, i.e., via IL-6, IL-8, and RANTES released from RSV-infected endothelial cells (our unpublished observations) or IL-8 and IL-1α released from RSV-infected epithelial cells (5, 33).

The increased binding rate of PMN to all three RSV-infected endothelial cell types under investigation resulted in an enhanced in vitro transmigration rate. Because PMN adhere and transmigrate always in a VCAM-1-independent manner, our finding that VCAM-1 was not up-regulated on RSV-infected lung endothelial cells should be without influence concerning the emigration rate of PMN. However, whether the RSV-induced ICAM-1 up-regulation mediating the increased adhesion of PMN to lung endothelial cells might be automatically involved in the transmigration process is still not known. Evidence accumulated that beside the well-known β_2-integrin-dependent transmigration process, a β_2-integrin-independent migration mechanism of PMN does exist in the lung (40, 41). Within the lung, this pathway is restricted to the lung capillaries. Recent data suggest that Gram-negative organisms induce a CD11/CD18-dependent PMN emigration out of the lung capillaries, whereas Gram-positive organisms elicit a CD11/CD18-independent emigration (42). However, in light of new published data this distinction obviously oversimplifies this multiform process. Which of these both transmigration mechanisms are actually operative is also in part dependent on the chronicity of reactions as well as on the various chemotaxins (43, 44). Thus, a CD18-independent transendothelial migration of PMN can be stimulated in vitro by the host-derived chemoattractants IL-8 and leukotriene B_4 (45). Because we used an IL-8 chemotaxin gradient in our in vitro transmigration model we suggest that cocultured PMN migrated in a CD18-independent way through the RSV-infected endothelial monolayer. In that case, the observed increased transmigration rate should be a direct consequence of the enhanced ICAM-1-mediated adhesion rate. However, future experiments have to address this point.

Concerning RSV infection there is currently no effective antiviral or anti-inflammatory treatment available. The analysis of the signal transduction pathways mediating the detrimental RSV-induced ICAM-1 cell surface expression may lead to the development of novel anti-inflammatory strategies. Therefore, we used pharmacological inhibitors to investigate which signaling pathways must be present in an active state to allow for RSV-induced up-regulation of ICAM-1 on HUVEC. Our data show that inhibition of PI3K by means of LY294002 reduced the RSV-induced ICAM-1 expression in a significant manner. Quite recently, Thomas et al. (34) reported that the RSV-induced apoptosis is delayed by activation of the PI3/Akt survival pathway. In this study, the PI3K inhibitor LY294002 was used at a concentration of 50 μM. We used the PI3K inhibitor at a nearly 10-times lower concentration, i.e., 6.4 μM, and observed no inhibitor-dependent cytotoxicity in RSV-infected HUVEC. Whether these divergent results are due to the different cell types used or result from the different inhibitor concentrations is still not known. Nevertheless, our data clearly show that PI3K activity is a prerequisite for RSV-induced ICAM-1 up-regulation. Furthermore, the inhibition of PKC- and PKA activity, before infection with RSV, diminished significantly the ICAM-1 up-regulation on HUVEC. Recently, studies performed by Monick et al. (36) showed that RSV activates multiple PKC isoforms in A549 lung epithelial cells, which subsequently leads to the activation of ERK. Three major types of MAPK cascades have been reported in mammalian cells, namely the ERK1/ERK2 cascade, the JNK/stress-activated protein kinase cascade, and the p38 kinase pathway. The activity of the MEK, ERK and p38 kinase in RSV-infected epithelial cells has been linked to RSV replication, IL-8 release, and posttranscriptional RANTES gene expression, respectively (35, 46, 47). Moreover, it was reported that expression of TNF-α and IL-1β in RSV-infected epithelial cells required the activation of the p38 MAPK pathway (48). Our data supply evidence that only the p38 MAPK pathway must be in an active state to allow for RSV-dependent ICAM-1 up-regulation. In summary, different protein kinases, i.e., PI3K, PKC, PKA, and p38 kinase, respectively, control the RSV-induced expression of ICAM-1 on HUVEC. Whether RSV-infected lung endothelial cells show an identical signal transduction pattern remains to be determined. Differences might exist as it was observed for HUVEC and primary endothelial cells (22) and rat pulmonary arterial vs rat pulmonary microvascular endothelial cells (49). Nevertheless, in comparison to HMVEC-L and HPAEC the RSV-induced expression of ICAM-1 was most prominent on HUVEC leading to the highest adhesion and transmigration rate of PMN. With regard to these data as well as their availability and reproduction, we suggest that HUVEC are a useful in vitro RSV infection model for analyzing the role of lung endothelial cells during an ongoing primary RSV infection. A comparison with primary lung endothelial cells, which has been done in our study will clarify the importance of novel results.

In summary, we conclude that pulmonary endothelial cells are target cells for productive RSV infection. Due to the up-regulation of ICAM-1 they might contribute to the detrimental accumulation of PMN into the RSV-infected lung. Therefore, similar to the RSV-infected lung epithelial cells they are intimately involved in the innate proinflammatory immune response.

Acknowledgments

We thank Bettina Polte for her excellent technical assistance in all the performed experiments.

Disclosures

The authors have no financial conflict of interest.

References

1. McIntosh, K. 1997. Respiratory syncytial virus. In *Viral Infections of Humans: Epidemiology and Control.* S. A. Evans and R. A. Kaslow, eds. Plenum Publishing, New York, p. 691–711.
2. Hall, C. B., and C. A. McCarthy. 2000. Respiratory syncytial virus. In *Principles and Practise of Infectious Diseases.* G. L. Mandell, J. E. Benett and R. Dolin, eds. Churchill Livingstone, Philadelphia, p. 1782–1801.
3. Falsey, A. R., and E. E. Walsh. 2000. Respiratory syncytial virus infection in adults. *Clin. Microbiol. Rev.* 13: 371–384.
4. Garofalo, R. P., and H. Haeberle. 2000. Epithelial regulation of innate immunity to respiratory syncytial virus. *Am. J. Respir. Cell Mol. Biol.* 23: 581–585.
5. Arnold, R., B. Humbert, H. Werchau, H. Gallati, and W. König. 1994. Interleukin-8, interleukin-6, and soluble tumor necrosis factor receptor type I release from a human pulmonary epithelial cell line (A549) exposed to respiratory syncytial virus. *Immunology* 82: 126–133.
6. Olszewska-Pazdrak, B., A. Casola, T. Saito, R. Alam, S. E. Crowe, F. Mei, P. L. Ogra, and R. P. Garofalo. 1998. Cell-specific expression of RANTES, MCP-1 and MIP-1α by lower airway epithelial cells and eosinophils infected with respiratory syncytial virus. *J. Virol.* 72: 4756–4764.
7. Harrison, A. M., C. A. Bonville, H. F. Rosenberg, and J. B. Domachowske. 1999. Respiratory syncytial virus-induced chemokine expression in the lower airways. *Am. J. Respir. Crit. Care Med.* 159: 1918–1924.
8. Arnold, R., H. Werchau, and W. König. 1995. Expression of adhesion molecules (ICAM- 1, LFA-3) on human epithelial cells (A549) after respiratory syncytial virus infection. *Int. Arch. Allergy Immunol.* 107: 392–393.
9. Arnold, R., and W. König. 1996. ICAM-1 expression and low-molecular-weight G-protein activation of human bronchial epithelial cells (A549) infected with RSV. *J. Leukoc. Biol.* 60: 766–771.
10. Matsuzaki, Z., Y. Okamoto, N. Sarashina, E. Ito, K. Togawa, and I. Saito. 1996. Induction of intercellular adhesion molecule-1 in human nasal epithelial cells during respiratory syncytial virus infection. *Immunology* 88: 565–568.
11. Arnold, R., B. König, H. Werchau, and W. König. 2004. Respiratory syncytial virus deficient in soluble G protein induced an increased proinflammatory response in human lung epithelial cells. *Virology* 330: 384–397.
12. Aherne, W., T. Bird, S. Court, P. Gardner, and J. McQuillin. 1970. Pathological changes in virus infections of the lower respiratory tract in children. *J. Clin. Pathol.* 23: 7–18.
13. Everard, M. L., A. Awarbrick, M. Wrightham, J. McIntyre, C. Dunkley, P. D. James, H. F. Sewell, and A. D. Milner. 1994. Analysis of cells obtained by bronchial lavage of infants with respiratory syncytial virus infection. *Arch. Dis. Child.* 71: 428–432.
14. Stark, J. M., V. Godding, J. B. Sedgwick, and W. W. Busse. 1996. Respiratory syncytial virus infection enhances neutrophil and eosinophil adhesion to cultured respiratory epithelial cells. *J. Immunol.* 156: 4774–4782.

15. Wang, S.-Z., H. Xu, A. Wraith, J. J. Bowden, J. H. Alpers, and K. D. Forsyth. 1998. Neutrophils induce damage to respiratory epithelial cells infected with respiratory syncytial virus. *Eur. Respir. J.* 12: 612–618.
16. Jaovisidha, P., M. E. Peeples, A. A. Brees, L. R. Carpenter, and J. N. Moy. 1999. Respiratory syncytial virus stimulates neutrophil degranulation and chemokine release. *J. Immunol.* 163: 2816–2820.
17. Abu-Harb, M., F. Bell, A. Finn, W. H. Rao, L. Nixon, D. Shale, and M. L. Everard. 1999. IL-8 and neutrophil elastase levels in the respiratory tract of infants with RSV bronchiolitis. *Eur. Respir. J.* 14: 139–143.
18. Haeberle, H. A., W. A. Kuziel, H.-J. Dieterich, A. Casola, Z. Gatalica, and R. P. Garofalo. 2001. Inducible expression of inflammatory chemokines in respiratory syncytial virus infected mice: role of MIP-1α in lung pathology. *J. Virol.* 75: 878–890.
19. Friedmann, H. M., E. J. Macarak, R. R. MacGregor, J. Wolfe, and N. A. Kefalides. 1981. Virus infection of endothelial cells. *J. Infect. Dis.* 143: 266–273.
20. Visseren, F. L., J. J. Bouwman, K. P. Bouter, R. J. Diepersloot, P. H. de Groot, and D. W. Erkelens. 2000. Procoagulant activity of endothelial cells after infection with respiratory viruses. *Thromb. Haemost.* 84: 319–324.
21. Salcedo, R., J. H. Resau, D. Halverson, E. A. Hudson, M. Dambach, D. Powell, K. Wasserman, and J. J. Oppenheim. 2000. Differential expression and responsiveness of chemokine receptors (CXCR1–3) by human microvascular endothelial cells and umbilical vein endothelial cells. *FASEB J.* 14: 2055–2064.
22. Haraldsen, G., D. Kvale, B. Lien, I. N. Farstad, and P. Brandtzaeg. 1996. Cytokine-regulated expression of E-selectin, intercellular adhesion molecule-1 (ICAM-1), and vascular cell adhesion molecule-1 (VCAM-1) in human intestinal microvascular endothelial cells. *J. Immunol.* 156: 2558–2565.
23. Jaffe, E. A., R. L. Nachmen, G. C. Becker, and C. R. Minick. 1973. Culture of human endothelial cells from umbilical veins. *J. Clin. Invest.* 52: 2745–2756.
24. Chen, T. R. 1977. In situ detection of mycoplasma contamination in cell cultures by fluorescent Hoechst 33258 stain. *Exp. Cell. Res.* 104: 255–262.
25. Ueba, O. 1978. Respiratory syncytial virus. I. Concentration and purification of the infectious virus. *Acta Med. Okayama* 32: 265–272.
26. Cannon, M. J. 1987. Microplaque immunoperoxidase detection of infectious respiratory syncytial virus in the lungs of infected mice. *J. Virol. Methods* 16: 293–301.
27. Arnold, R., M. Seifert, K. Asadullah, and H. D. Volk. 1999. Crosstalk between keratinocytes and T lymphocytes via Fas/FasL interaction: modulation by cytokines. *J. Immunol.* 162: 7140–7147.
28. Mul, F. P. J., A. E. M. Zuurbier, H. Janssen, J. Calafat, S. van Wetering, P. S. Hiemstra, D. Roos, and P. L. Hordijk. 2000. Sequential migration of neutrophils across monolayers of endothelial and epithelial cells. *J. Leukoc. Biol.* 68: 529–537.
29. Wang, S. Z., P. G. Hallsworth, K. D. Dowling, J. H. Alpers, J. J. Bowden, and K. D. Forsyth. 2000. Adhesion molecule expression on epithelial cells infected with respiratory syncytial virus. *Eur. Respir. J.* 15: 358–366.
30. Scholz, D., B. Devaux, A. Hirche, B. Pötzsch, B. Kropp, W. Schaper, and J. Schaper. 1996. Expression of adhesion molecules is specific and time-dependent in cytokine-stimulated endothelial cells in culture. *Cell Tissue Res.* 284: 415–423.
31. Ledebur, H. C., and T. P. Parks. 1995. Transcriptional regulation of the intercellular adhesion molecule-1 gene by inflammatory cytokines in human endothelial cells. *J. Biol. Chem.* 270: 933–943.
32. Nilson, E. M., F.-E. Johansen, F. L. Jahnsen, K. E. A. Lundin, T. Scholz, P. Brandtzaeg, and G. Haraldsen. 1998. Cytokine profiles of cultured microvascular endothelial cells from human intestine. *Gut* 42: 635–642.
33. Patel, J. A., M. Kunimoto, T. C. Sim, R. Garofaldo, T. Eliott, S. Baron, O. Ruuskanen, T. Chonmaitree, P. L. Ogra, and F. Schmalstieg. 1995. Interleukin-1α mediates the enhanced expression of intercellular adhesion molecule-1 in pulmonary epithelial cells infected with respiratory syncytial virus. *Am. J. Respir. Cell Mol. Biol.* 13: 602–609.
34. Thomas, K. W., M. M. Monick, J. M. Staber, T. Yarovinsky, A. B. Carter., and G. W. Hunninghake. 2002. Respiratory syncytial virus inhibits apoptosis and induces NF-κB activity through a phosphatidylinositol 3-kinase-dependent pathway. *J. Biol. Chem.* 277: 492–501.
35. Kong, X., H. S. Juan, A. Behera, M. E. Peeples, J. Wu, R. F. Lockey, and S. S. Mohapatra. 2004. ERK-1/2 activity is required for efficient RSV infection. *FEBS Lett.* 559: 33–38.
36. Monick, M. M., J. M. Staber, K. W. Thomas, and G. W. Hunninghake. 2002. Respiratory syncytial virus infection results in activation of multiple protein kinase C isoforms leading to activation of mitogen-activated protein kinase. *J. Immunol.* 166: 2681–2687.
37. Chini, B. A., M. A. Fiedler, L. Milligan, T. Hopkins, and J. M. Stark. 1998. Essential roles of NF-κB and C/EBP in the regulation of intercellular adhesion molecule-1 after respiratory syncytial virus infection of human respiratory epithelial cell cultures. *J. Virol.* 72: 1623–1626.
38. Chang, C.-H., Y. Huang, and R. Anderson. 2003. Activation of vascular endothelial cells by IL-1α released by epithelial cells infected with respiratory syncytial virus. *Cell Immunol.* 221: 37–41.
39. Doyle, N. A., S. D. Bhagwan, B. B. Meek, G. J. Kutkoski, D. A. Steeber, T. F. Tedder, and C. M. Doerschuk. 1997. Neutrophil margination, sequestration and migration in the lungs of L-selectin-deficient mice. *J. Clin. Invest.* 99: 526–533.
40. Yamamoto, T., O. Kajikawa, T. R. Martin, S. R. Sharar, J. M. Harlan, and R. K. Winn. 1998. The role of leukocyte emigration and IL-8 on the development of lipopolysaccaride-induced lung injury in rabbits. *J. Immunol.* 161: 5704–5709.
41. Burns, J. A., T. B. Issekutz, H. Yagita, and A. C. Issekutz. 2001. The $\alpha_4\beta_1$ (very late antigen (VLA)-4), CD49d/CD29) and $\alpha_5\beta_1$ (VLA-5, CD49e/CD29) integrins mediate β_2 (CD11/CD18) integrin-independent neutrophil recruitment to endotoxin-induced lung inflammation. *J. Immunol.* 166: 4644–4649.
42. Doerschuk, C. M., S. Tasaka, and Q. Wang. 2000. CD11/CD18-dependent and -independent neutrophil emigration in the lungs: how do neutrophils know which route to take? *Am. J. Respir. Cell Mol. Biol.* 23: 133–136.
43. Kumasaka, T., N. A. Doyle, W. M. Quinlan, L. Graham, and C. M. Doerschuk. 1996. Role of CD11/CD18 in neutrophil emigration during acute and recurrent *Pseudomonas aeruginosa*-induced pneumonia in rabbits. *Am. J. Pathol.* 148: 1297–1305.
44. Morland, C. M., B. J. Morland, P. J. Darbyshire, and R. A. Stockley. 2000. Migration of CD18-deficient neutrophils in vitro: evidence for a CD18-independent pathway induced by IL-8. *Biochim. Biophys. Acta* 1500: 70–76.
45. Mackarel, A. J., K. J. Russell, C. S. Brady, M. X. FitzGerald, and C. M. O'Connor. 2000. Interleukin-8 and leukotriene B_4, but not formylmethionyl-leucylphenylalanine, stimulate CD18-independent migration of neutrophils across human pulmonary endothelial cells in vitro. *Am. J. Respir. Cell Mol. Biol.* 23: 154–161.
46. Chen, W., M. M. Monick, A. B. Carter, and G. W. Hunninghake. 1999. Activation of ERK2 by respiratory syncytial virus in A549 cells is linked to the production of interleukin 8. *Exp. Lung Res.* 26: 13–26.
47. Pazdrak, K., B. Olszewska-Pazdrak, T. Liu, R. Takizawa, A. R. Brasier, R. P. Garofalo, and A. Casola. 2002. MAPK activation is involved in postranscriptional regulation of RSV-induced RANTES gene expression. *Am. J. Physiol.* 283: L364–L372.
48. Meusel, T. R., and F. Imani. 2003. Viral induction of inflammatory cytokines in human epithelial cells follows a p38 mitogen-activated protein kinase-dependent but NF-κB-independent pathway. *J. Immunol.* 171: 3768–3774.
49. Wang, Q., G. R. Pfeiffer II, T. Stevens, and C. M. Doerschuk. 2002. Lung microvascular and arterial endothelial cells differ in their response to intercellular adhesion molecule-1 ligation. *Am. J. Respir. Crit. Care Med.* 166: 872–877.